

High-order synchronization, transitions, and competition among Arnold tongues in a rotator under harmonic forcing

David García-Álvarez,* Aneta Stefanovska, and Peter V.E. McClintock
Department of Physics, Lancaster University, Lancaster LA1 4YB, United Kingdom

(Dated: March 12, 2008)

We consider a rotator whose equation of motion for the angle θ consists of the zeroth and first Fourier modes. Numerical analysis based on the trailing of saddle-node bifurcations is used to locate the $n:1$ Arnold tongues where synchronization occurs. Several of them are wide enough for high-order synchronization to be seen in passive observations. By sweeping the system parameters within a certain range, we find that the stronger the dependence of $\dot{\theta}$ on θ , the wider the regions of synchronization. Use of a synchronization index reveals a vast number of very narrow $n:m$ Arnold tongues. A competition phenomenon among the tongues is observed, in that they “push” and “squeeze” one another: as some tongues widen, others narrow. Two mechanisms for transitions between different $n:m$ synchronization states are considered: slow variation of the driving frequency, and the influence of low-frequency noise on the rotator.

PACS numbers: 05.45.Xt, 45.20.dc, 05.40.Ca, 87.19.Hh

I. INTRODUCTION

When two or more oscillatory processes are coupled, there exists the possibility of their becoming synchronized. Where their autonomous frequencies are different but close, synchronization is understood as the adjustment of those frequencies as a result of coupling. Even when such systems operate on different timescales, synchronization may still appear as an adjustment of their frequencies to an integer ratio, an effect known as *high-order synchronization* or synchronization of order $n:m$.

Synchronization of order $n:m$ has been extensively studied, both experimentally and theoretically (cf. [1] for a review). For instance, Simonet and co-workers [2] investigated a ruby nuclear magnetic resonance laser with delayed feedback. The undriven laser exhibited periodic oscillations of light intensity at a frequency $\nu_0 \simeq 40$ Hz. An external periodic voltage, either sinusoidal or square-wave, was then added in the feedback loop. In both cases, synchronizations of different order $n:m$ were observed. Another example is the electrical rotator consisting of a Josephson junction, shunted by a capacitor, and fed with a constant external current. Experiments show that this system can be synchronized when a periodic driving current is applied, or where two junctions are coupled [3]. There are many additional examples.

Synchronization has also been observed extensively in biology. One example is the cardiorespiratory system, considered in the pioneering works by Kenner et al, Hildebrandt and Raschke [4]. Schäfer and co-workers [5] proposed the synchrogram as a tool to visualize cardiorespiratory synchronization. When plotting the instantaneous respiratory phase at the occurrence of a heartbeat versus time, they found horizontally striped plots for some

subjects, thereby revealing $n:1$ synchronization between heart and respiration. Toledo et al [6] showed that the probability of such synchronization happening by chance was extremely small. In measurements on anaesthetised rats, Stefanovska et al [7] observed lengthy synchronization epochs, and transitions from one ratio to another. They suggested that such transitions might be useful in monitoring depth of anaesthesia.

There are several nonlinear models yielding $n:m$ synchronization. Arnold proposed [8] a map of the circle into itself, obtaining synchronization “tongues” and calculating their widths in the approximation of small coupling. In fact, any orientation-preserving homeomorphism $h:S^1 \rightarrow S^1$ of the circle into itself presents such regions of $n:m$ locking [9, 10]. Integrate-and-fire models provide several examples of Arnold tongues [11]. High-order synchronization regions were also obtained by Glass and Sun [12] for an impulse-driven Poincaré oscillator. Schilder and Peckham [13] treated Arnold tongues numerically, and they obtained tongues for the system of two coupled Van der Pol oscillators; here the tongues are quite narrow, so that the probability of locking in a real, noisy system, would therefore be very small. Simonet and co-workers proposed a model [2] that reproduced the synchronizations observed in the laser. For cardiorespiratory synchronization, Kotani et al [14] developed a model, based on those of DeBoer et al [15] and Seidel and Herzel [16], which is supported on both physiological and mathematical principles. The model involves a somewhat complicated system consisting of several oscillators and interactions, and includes some non-analytic parts (integrate-and-fire). Because of technical difficulties encountered when tackling nonlinear models, the deep mechanisms through which synchronization takes place are not yet understood in general, so that there is still no way of predicting which equations, and which values of their parameters, will or will not yield synchronization.

*Electronic address: d.garcia-alvarez@lancaster.ac.uk

The present paper has two main purposes. First we present a systematic study of high-order synchronization in a particularly simple system, a rotator under harmonic forcing, for which we can establish the roles played by each of its parameters in synchronization. Although we study a specific system, and although the deep mechanisms responsible for synchronization are not unveiled in this paper, we report below two results that we believe will be useful in the quest for those deep mechanisms: we show that the main Arnold tongues are wider when $\dot{\theta}$ depends more strongly on θ ; and that competition occurs between synchronization regions. Our second purpose is to discuss and explore two possible mechanisms giving rise to an extensively observed phenomenon: transitions between the different $n:m$ synchronization ratios. The mechanisms considered here arise from time variability. We will also discuss briefly why time variability hinders the analysis of synchronization in experimental data.

The paper is organized as follows: In Sec. II we introduce the simple rotator whose synchronization properties are to be considered. Sec. III discusses how its regions of $n:1$ and $n:m$ synchronization are identified and reports the main results obtained under stationary conditions, including the observation of competition between the tongues. Time variability and its effect on transitions between different synchronization states is discussed in Sec. IV. Sec. V summarizes the main conclusions.

II. THE SYSTEM

The generic equation for the angle θ of a rotator without external interaction is

$$\dot{\theta} = f(\theta),$$

where f is a 2π -periodic function [17]. Therefore, such a system can be studied systematically by considering functions f up to a certain number k of harmonics, and allowing a bigger number $k+1$ of harmonics at the next stage of the study. In this paper, we start the study for a function consisting of the zero harmonic (the “constant force”, thanks to which a rotator has the features of a self-sustained oscillator) and the first harmonic. By means of a translation in the value of θ , it can always be written as

$$\dot{\theta} = a_0 + a_1 \cos \theta, \quad (1)$$

with a_0 and a_1 constants, where (1) is an Adler-type equation [19]. We assume $a_0 > |a_1|$ so that, in the absence of interaction (nothing is added to (1)), the angle θ continuously increases. For a_0 much bigger than a_1 , θ increases at an almost constant rate. For a_1 close to a_0 , however, $\dot{\theta}$ varies strongly with θ . We show that (1) can synchronize to an external forcing, exhibiting a wide variety of Arnold tongues, and we discuss the processes that may be responsible for transitions between different $n:m$ synchronization ratios.

The equations for the overdamped pendulum, and the overdamped Josephson junction, are of just this type. The equation of motion of a pendulum driven by a constant torque K is described by

$$\ddot{\Psi} + \gamma \dot{\Psi} + \kappa^2 \sin \Psi = \frac{K}{I}, \quad (2)$$

where κ is the frequency of small oscillations, $\gamma > 0$ is the damping constant, and I is the moment of inertia.

In a resistively shunted Josephson junction, the current is a sum of three contributions: a superconducting current $I_c \sin \Psi$, a current V/R through the resistance, and a capacitance current $\dot{V}C$. The parameter I_c is called the critical supercurrent of the junction. The relationship between the potential V and the “angle” Ψ is given by the Josephson formula

$$\dot{\Psi} = \frac{2e}{\hbar} V, \quad (3)$$

where e is the electronic charge. Summation of the three terms yields the equation for a junction fed with an external current I

$$I = I_c \sin \Psi + \frac{\hbar}{2eR} \frac{d\Psi}{dt} + \frac{C\hbar}{2e} \frac{d^2\Psi}{dt^2}. \quad (4)$$

Equations (2) and (4) coincide. In the overdamped limit, when the term with the second derivative can be neglected – in the case of the Josephson junction, this means that there is no capacitor in the circuit – these equations reduce to the one that we study in this paper (1). Thus the results that we obtain below will be applicable to the overdamped pendulum and the overdamped Josephson junction.

As (1) is analytically integrable, we find that the frequency for the non-interacting rotator is

$$\nu_0 = \frac{1}{2\pi} \sqrt{a_0^2 - a_1^2}. \quad (5)$$

We now consider the effect of an external harmonic force on the rotator

$$\dot{\theta} = a_0 + a_1 \cos \theta + B \sin(\omega t), \quad (6)$$

with $B \geq 0$. This equation applies to a number of situations in nature. In the case of a Josephson junction, Eq. (6) describes when the system is fed with a continuous intensity plus a harmonic one. In relation to cardiorespiratory synchronization, (6) can be regarded as a very simple model in which the rotator (1) models the heart, and the addition of the harmonic component models its interaction with respiration [20]. Eq. (6) has been studied [1] for large amplitudes B of the harmonic component. However, we are interested here in the Arnold tongues down to very small driving amplitude, in order that we can also apply the results to the weakly coupled rotator.

Eq. (6) defines a circle map with the following prescription: let us call t_i the time at which the external driving

is at its i^{th} maximum. We define $\theta_i \equiv \theta(t_i)$. As (6) is a first-order differential equation and we have an initial condition $\theta(t_i)$, we could integrate to obtain $\theta(t)$. Let t_{i+1} be the time at which the external driving is at its $i+1$ maximum, and let $\theta_{i+1} \equiv \theta(t_{i+1})$. That is how we have the map $h: S^1 \rightarrow S^1$ defined as $\theta_{i+1} = h(\theta_i)$. We would therefore expect the existence of Arnold tongues [9, 10].

III. SYNCHRONIZATION AND ARNOLD TONGUES

A. Synchronization of a rotator driven by an external periodic force

Now we introduce the concept of $n:m$ synchronization that will be used in this work. Suppose we have a rotator driven by a T_E -periodic external action

$$\begin{aligned} \dot{\theta} &= f(\theta) + g(t), & \text{with} \\ f(\theta + 2\pi) &= f(\theta) \quad \forall \theta, & g(t + T_E) = g(t) \quad \forall t. \end{aligned}$$

Then, any T -periodic motion of θ , $\theta(t+T) = \theta(t) \bmod 2\pi$, must have a period that is a multiple of the driving period. Let $m \in \mathbb{N}$ be such that $T = m T_E$. Let $n \in \mathbb{N} \cup \{0\}$ be the number of times that the angle crosses $\theta = 0 \bmod 2\pi$ with $\dot{\theta} > 0$ in one of its periods $T = m T_E$. We then say that the rotator is $n:m$ synchronized to the external driving g . The synchrogram consists then of *horizontal lines*, albeit not necessarily equally spaced. Note that any periodic motion of the forced rotator automatically implies $n:m$ locking to the external action for some n and m .

B. Saddle-node bifurcation

Putting the above definition of $n:m$ synchronization into mathematical terms, we say that the rotator gets synchronised $n:m$ to the external force if there exists a stable root (zero) for the function

$$h_{nm}(\theta) \equiv h^m(\theta) - 2\pi n - \theta, \quad (7)$$

where h^m stands for the return map h composed with itself m times. In general, if h_{nm} has two or more roots, there is at least a stable fixed point. Regardless of the initial condition, the trajectory is attracted towards a stable fixed point. The function h_{nm} depends, of course, on the parameters of (6), so it changes as we vary the external driving frequency ω . At the moment of transition from two zeros to no zero, there is only one root, on which h_{nm} is tangent to the horizontal axis, this single zero is a half-stable fixed point. At this moment, a *saddle-node bifurcation* takes place.

Obtaining the borders of the Arnold tongues therefore involves retrieving the two driving frequencies at which

the saddle-node bifurcation takes place for different values of the driving amplitude B . For this purpose a *continuation software* was written in C. The first step was to obtain the Poincaré return map h , so the interval $[0, 2\pi]$ was divided into many points. At each of these, the function h^m was obtained by integration of the differential equation (6) with the fourth-order Runge-Kutta method, thereby obtaining $h_{nm}(\theta) = h^m(\theta) - 2\pi n - \theta$. For given values of B and ω , we know that we are inside the tongue if h_{nm} has two or more roots, and outside if h_{nm} has no zeros. Hence, for a given value of B , we can trace the left and right values of ω at which the saddle-node bifurcation takes place, up to the desired precision. We start with zero driving amplitude, $B = 0$; for this value the tongue consists of only one point $\omega = m \omega_0/n$ – this will not be forced when we study the bifurcations in the “flexible” way for very narrow tongues, see Section III F. For the next value of the coupling (positive but close to 0), we start from $\omega = m \omega_0/n$ and look for the two bifurcation points. Then, for sequentially increasing values of B , we first guess approximately the bifurcation points on the left and right boundaries by linear extrapolation from the two former bifurcation frequencies in each case. Starting from this guessed value, the programme looks for the correct bifurcation point. In some tongues and for small values of B , the synchronization region is so narrow that the programme cannot retrieve the bifurcation points. In such cases, the programme skips this value of B , goes to the next B , and sets the starting point (the “guessed value” of the bifurcation frequency) based on the former bifurcation points that were successfully retrieved.

C. The $n:1$ synchronization regions

We obtained the first $n:1$ tongues for three combinations of parameters (a_0, a_1) that, according to (5), yield the same autonomous frequency for the rotator $\nu_0 \simeq 1.0811$: (7.08116, 2), (9.85714, 7.14286) and (16.46637, 15). Note that dimensionless units are used for all variables throughout this paper. The results are plotted in Fig. 1. The tongues with $m > 1$ are very narrow and the programme fails to retrieve them by the method of seeking the saddle-node bifurcations. Later we will use other less accurate methods for the high-order tongues. As often reported in the literature [8], the widest tongues are those for $m = 1$. For our system (6), as n increases, the widths of the $m = 1$ tongues decrease and the tongues become closer to one another. A point of interest here is that there are several Arnold tongues that are wide enough to be seen, not only by seeking them in a tuned experiment, but also through passive observations in the presence of noise, e.g. the cardiovascular system [5, 7, 22].

In our second parameter set, a_1 is bigger than in the first set, and longer again in the third set compared to

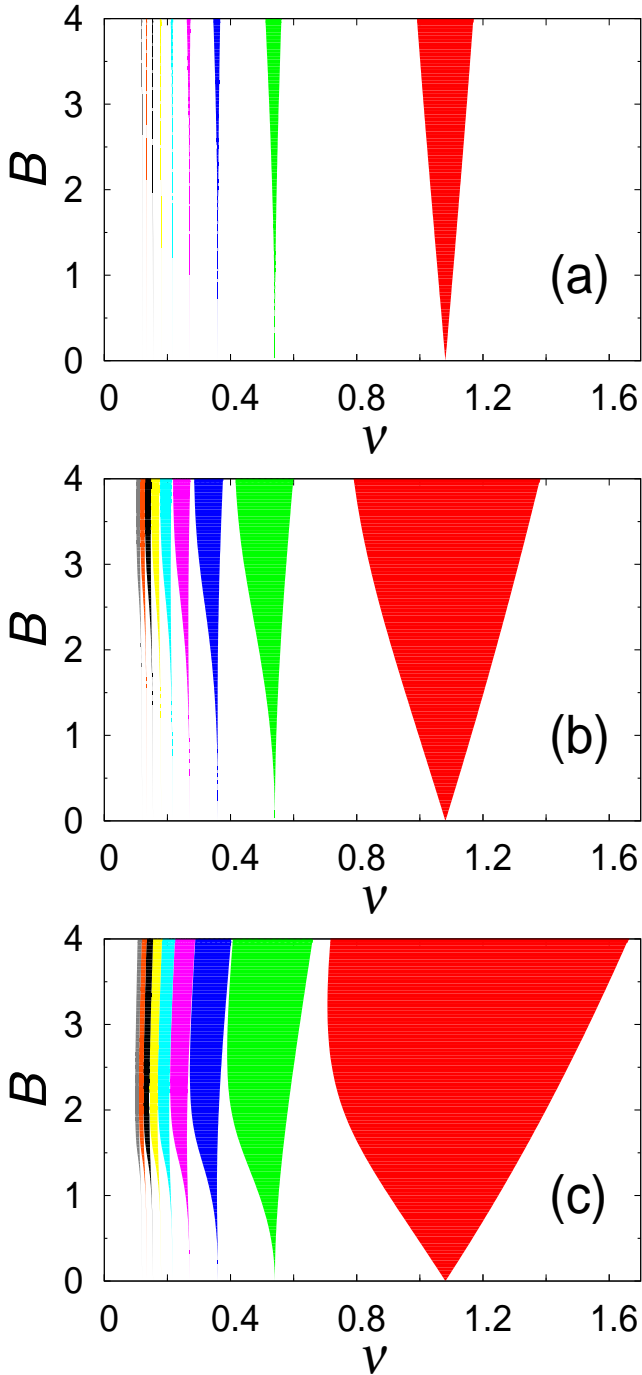


FIG. 1: (colour online) Arnold tongues for the externally-driven rotator (6), with parameters (a_0, a_1) equal to: (7.08116, 2) in (a); (9.85714, 7.14286) in (b); and (16.46637, 15) in (c). The frequency ν and amplitude B of the external driving are plotted on the abscissa and ordinate axes respectively. The tongues are $n:1$, with n increasing from 1 to 9 as we move from right to left.

the second one. Thus, the value of $\dot{\theta}$ depends much more strongly on θ as we move from (a) to (c) in Fig. 1, al-

though the frequency ν_0 remains the same. The effect on the Arnold tongues is immediately evident on comparing the three plots in Fig. 1: the tongues become markedly wider, thereby favouring synchronization. We may therefore conjecture that a strong dependence of the instantaneous frequency on angle (for the uncoupled rotator) may help high order synchronization.

In order to check this conjecture more thoroughly, we fix the value of the driving amplitude B to 1.5, and we compute the widths of the tongues at $B = 1.5$ for different values of the parameters a_0 and a_1 . We swept a_0 from 2 to 30, and a_1 from 2 to (almost) a_0 . In order to compute the width of the tongues, the code was modified, so that the two driving frequencies at which the saddle-node bifurcations take place were computed only for this value of B . Starting from $\omega = m\omega_0/n$, we trailed the bifurcation points first with small precision, then with a greater one, recursively up to the desired precision. We plot in Fig. 2 the widths of the tongues at $B = 1.5$ versus the autonomous frequency ν_0 and the parameter a_1 (to which a_0 is related through (5)). In the figure we see that, for the same autonomous frequency ν_0 , the widths of the tongues dramatically increase with a_1 , confirming the conjecture that a strong dependence of $\dot{\theta}$ on θ (for the uncoupled rotator) favours synchronization. Regarding this conjecture, it would be very interesting to add higher harmonics to (1) and to study how the widths of the tongues for the driven rotator change. Nevertheless, in this case, the frequency ν_0 of the isolated rotator is not an elementary function, so it would perhaps be more convenient to calculate this frequency numerically.

D. Use of the synchronization index

As mentioned above, the tongues with $m > 1$ are very narrow and the programme fails to retrieve them by the method of seeking the saddle-node bifurcations. In order to obtain the synchronization regions in such cases, we have been obliged to use other (albeit less accurate) approaches. The first one is via a synchronization index: we generated data by numerical integration of Eq. (6) with the fourth-order Runge-Kutta method; and we analysed them as though they were experimental data, by computing their synchronization index. With the definition of synchronization we mentioned at the beginning, it is natural to quantify it by how close the following index [14] is to zero

$$H_{mn} = \frac{1}{2\pi m(L-n)} \left| \sum_{i=n+1}^L (\Phi_i - \Phi_{i-n} - 2\pi m) \right|, \quad (8)$$

where L is the total number of crossings of $\theta = 0 \bmod 2\pi$ with $\dot{\theta} > 0$, and Φ is the phase of the external action when the i^{th} crossing occurs.

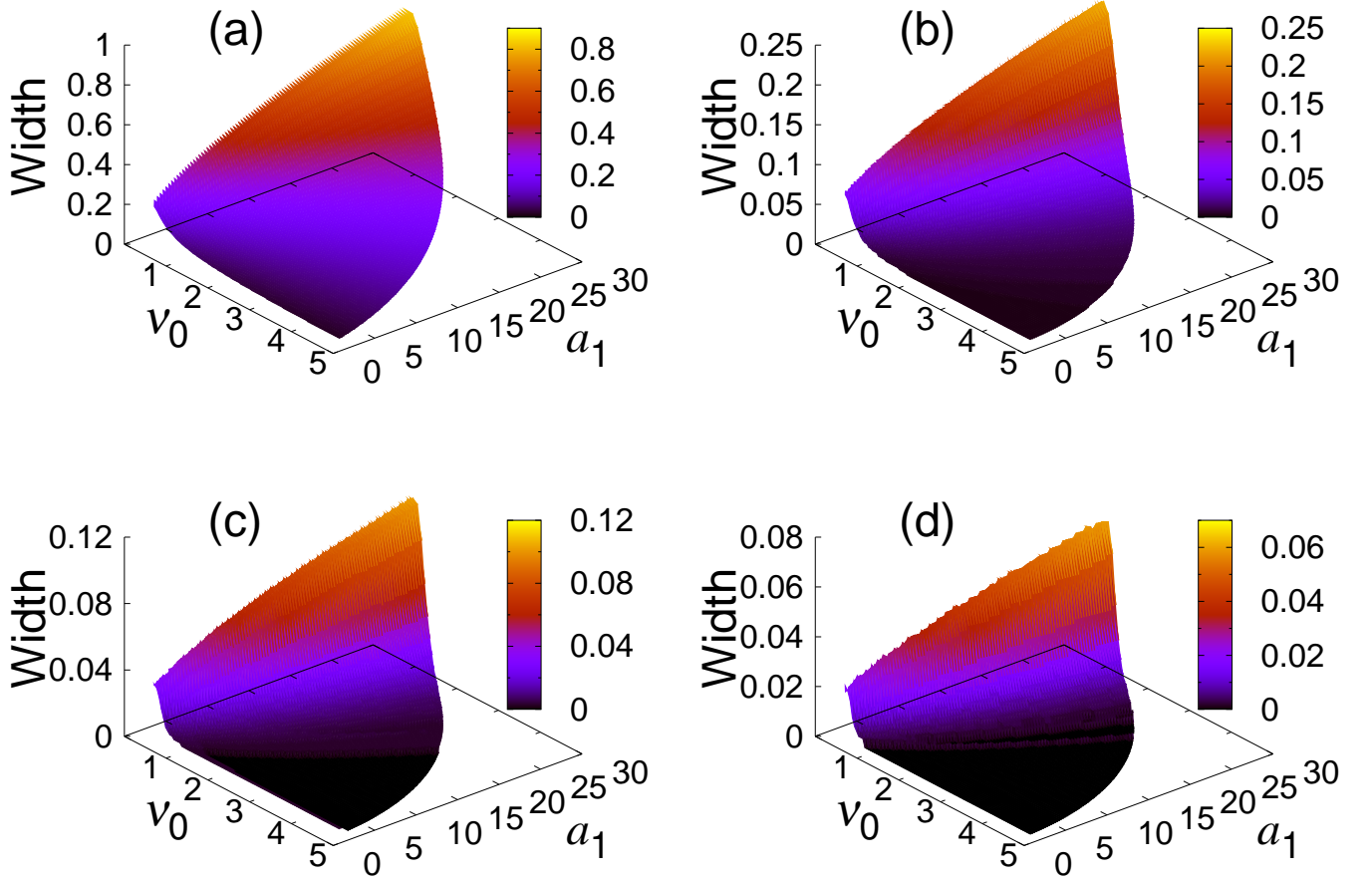


FIG. 2: (color online) Widths of the Arnold tongues as functions of parameters a_1 and ν_0 : (a) 1:1; (b) 1:2; (c) 1:3; and (d) 1:4. They are expressed in units of the driving frequency ν , at driving amplitude $B = 1.5$. Note the differences in ordinate scale.

E. The $n:m$ synchronization regions

To illustrate the $n:m$ synchronization regions, we again plot the driving frequency ν on the horizontal axis, and the coupling or driving amplitude B on the vertical axis. The horizontal axis was divided into 5,000 points, and the vertical one into 30 points. For each of the 150,000 corresponding pairs of points, the Eq. (6) was integrated. The first 60 zero-positive crossings were discarded to remove transients. The maximum accepted value of the index H_{mn} (8) for a point to be considered as belonging to the $n:m$ Arnold tongue was 0.0005.

Fig. 3 plots the results obtained for two of the parameter sets. We only plotted those tongues whose horizontal widths were larger than 0.00026 for at least one value of the coupling B (an arbitrary cutoff chosen by trial and error, in order to plot neither too many nor too few tongues) [23]. We can see in that figure the vast variety of synchronization regions that the system yields. There are even some on this Fig. with $m = 10$, the highest value

of m that we trailed. As we reduce the lower cutoff of the width criterion, many new tongues arise in the plot. The effect of synchronization with the external action can be inferred from the fact that these tongues are not vertical lines, but curved.

Furthermore, comparison of Figs. 3(a) and 3(b) shows that the tongues become closer to vertical straight lines for smaller a_1 , implying that synchronization is more and more a matter of fine tuning of the external driving frequency rather than of the interaction of the rotator with the external action. This phenomenon provides further confirmation of our hypothesis that a strong dependence of instantaneous frequency on angle (for the uncoupled rotator) helps high-order synchronization.

F. Competition among the tongues

The curving of the high-order tongues in Fig. 3(a) can be attributed to the occurrence of *competition among*

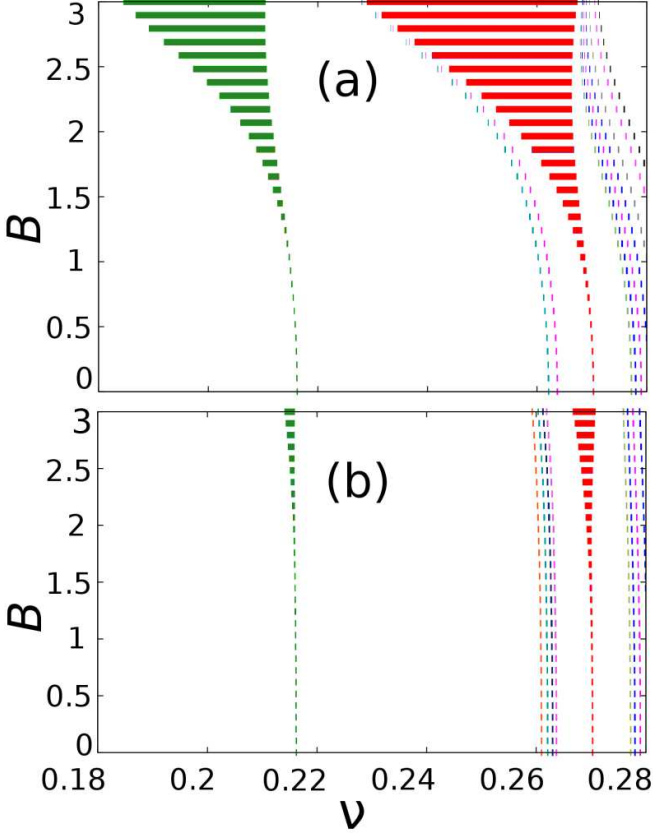


FIG. 3: (colour online) Detail of the synchronization regions inside a small interval. The parameters (a_0, a_1) are: (a) (9.85714, 7.14286); (b) (7.08116, 2). The tongues are, from left to right: (a): 5:1, 33:8, 41:10, 4:1, 39:10, 35:9, 31:8, 27:7, 23:6, 19:5, and 34:9; (b): 5:1, 29:7, 33:8, 37:9, 41:10, 4:1, 39:10, 35:9, 31:8, and 27:7

tongues: in this case the 4:1 tongue widens as the coupling increases and “pushes” the high-order tongues. Our circle map h is always invertible, because equation (6) can be integrated with reversed time. Therefore, Lemma 1.5 in [10] says that the Arnold tongues cannot overlap. That is the basis on which we argue that there must be competition among the tongues.

We note here several signs of such competition. First, the 37:9 tongue appears in Fig. 3(b) but not in 3(a), because it is narrower there. We can interpret this effect as 33:8 and 41:10 *squeezing* it for the set of parameters used in 3(a).

In the same way, the widths for 33:8 and 41:10 obtained via the synchronization index in Fig. 3(a) are of the order of 10^{-4} at $B \rightarrow 0$, and of the order of 10^{-5} at $B = 3$. Nevertheless, the width of the synchronization region as $B \rightarrow 0$ must tend exactly to zero. As indicated above, the computation of Arnold tongues via a synchronization index (using (8) in our case) is less accurate. Because of this evident contradiction between the obtained width

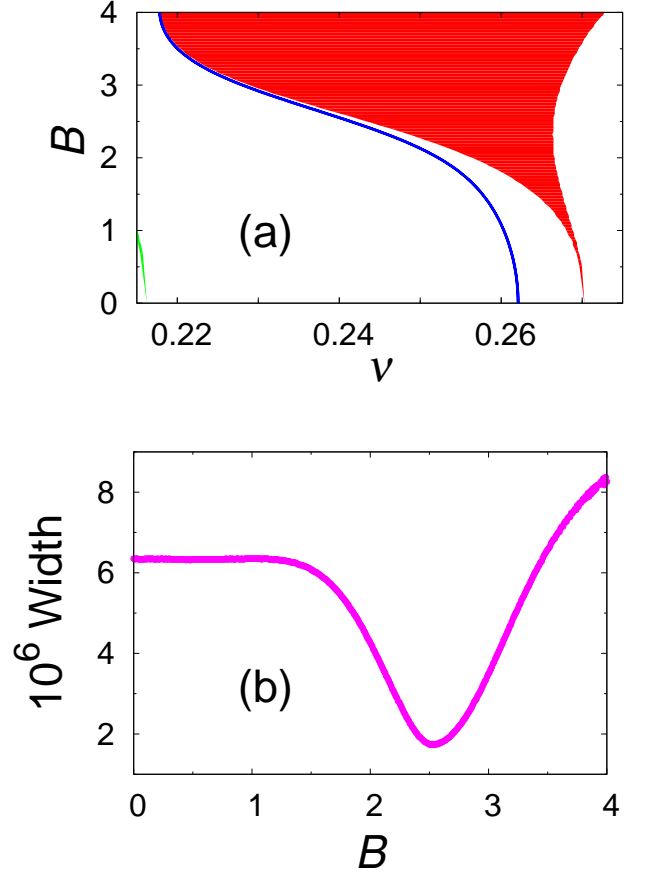


FIG. 4: (colour online) (a) Tongues 4:1 (right) and 33:8 (second from the right) for parameters $(a_0, a_1) = (9.85714, 7.14286)$. For clarity, the width of the 33:8 tongue in (a) is shown as larger than it really is: this plot is just intended to show the location. (b) Width of the 33:8 tongue, plotted as a function of the driving amplitude B . The location of the 33:8 tongue in (a), and its width in (b), were obtained by trailing the bifurcations in their “flexible” meaning, using a threshold of 0.001.

of the tongue as $B \rightarrow 0$ (width bigger than zero) and the actual value of the width (strictly zero), we need a more defined approach. The first try was to obtain the bifurcation points with the first programme but it was impossible: although we set a high precision, we failed to find any zeros for the function h_{nm} .

That is why we are introducing the third method of obtaining approximately Arnold tongues for tricky cases like this one: *trailing the bifurcations in their “flexible” meaning*. Instead of considering that we are inside the tongue when h_{nm} has a stable zero, we relax the condition and just ask h_{nm} to have an “almost (half stable) zero”, defined as a point where h_{nm} takes an absolute value smaller than a threshold (set here to be 0.001). It means that, if we measure the angle of the rotator at the times

when the external action has a maximum, this angle will stay for a long time around this minimum (or rather, minimum in absolute value). What happens afterwards depends on the behaviour of h_{nm} . If h_{nm} increases quickly (in absolute value) when we separate from the minimum, the angle will slip and come back promptly to the minimum (modulus 2π). If h_{nm} is still very small when we separate from the minimum, the angle will have a slow drift when iterating h_{nm} so, in practice, the system will be regarded as synchronized, unless the measurements are very precise.

The tongue 33:8 obtained this way is plotted in Fig. 4(a), together with the 4:1 tongue obtained before. In Fig. 4(b) we plotted the width of the 33:8 tongue as a function of the driving amplitude B . Because of the “flexible” way of obtaining the tongue, its width tends to a value bigger than zero as $B \rightarrow 0$. The explanation is simple: without any driving ($B = 0$) there is no interaction, so the only possibility of having an apparent synchronization – not true synchronization, as there is no interaction – is to tune the external frequency to the value $m\nu_0/n$. This frequency is the only point of the Arnold tongue in the limit $B \rightarrow 0$. The function h_{nm} is there constantly equal to zero. If we make the external frequency slightly different from $m\nu_0/n$, with $B = 0$, the values returned by the function h_{nm} will still be very small, so many of them will be below the threshold; that is the reason why the obtained width of the tongue in the limit $B \rightarrow 0$ is bigger than zero. Of course, this “flexible” method is not completely accurate, and it gives the apparent contradiction above. Nevertheless, we are using this method only to obtain qualitative conclusions, by *comparing* results all obtained with the same method. So we believe that the conclusions remain valid.

As we can see from Fig. 4(b), the width of the 33:8 tongue is more or less constant for B near zero, and then it starts dropping at around $B = 1.5$. Looking at Fig. 4(a), we may interpret $B = 1.5$ as the point where the 4:1 tongue has approached 33:8 enough to start squeezing it. The width of 33:8 reaches a minimum at $B = 2.5$ and then it increases. In Fig. 4(a), $B = 2.5$ is more or less the point where 4:1 switches from being concave (concave from outside) to convex, so it is consistent with the fact that the width of 33:8 starts increasing at this point: let us say that, before this point, 4:1 was “invading” 33:8; from this point, 33:8 “starts recovering from 4:1’s invasion”, so 33:8 gains space (width) and 4:1 switches from being concave to be convex (of course, there are, mathematically speaking, an infinite number of tongues between 33:8 and 4:1, but 4:1 is the most dominant in the area so it is the main influence).

The cases discussed above reveal clear signs of the effect of competition among tongues; the existence of such competition was predicted at the outset on strictly theoretical grounds.

IV. TIME VARIABILITY AND TRANSITIONS BETWEEN DIFFERENT SYNCHRONIZATION EPOCHS

Transitions in time between states of different $n:m$ synchronization ratios have often been observed experimentally [5, 7, 22, 24]. We now consider in turn two mechanisms that may give rise to such transitions in our system (6): (i) variability of the driving frequency, and (ii) low-frequency noise. The latter is mathematically equivalent to slow variations of the autonomous frequency of the rotator. Both mechanisms correspond to time variability, and they can coexist.

A. Variability of the driving frequency

We again simulated the system (6), but modified such that we replaced $B \sin(\omega t)$ with $B \sin(\Phi(t))$, and varied the instantaneous frequency $\dot{\Phi}(t)$ linearly in time

$$\dot{\Phi}(t) = a t + b; \quad \Phi(t) = \frac{1}{2} a t^2 + b t. \quad (9)$$

The choice of a linear variation was arbitrary, in the interests of clarity. With the parameters of (6) chosen to be $(a_0, a_1) = (9.85714, 7.14286)$, $B=4$, we slowly swept $\dot{\Phi}(t)/2\pi$ from 0.1 to 1.3 in a total time of 72,000. Fig. 5 shows $n:1$ synchronization epochs corresponding to the times when the external instantaneous frequency is inside an Arnold tongue. As n decreases, the synchronization epochs last longer, and the transition regions widen. That is because, as mentioned above, the Arnold tongues are then wider and further separated. The $n:2$ epochs are also observed from the synchrograms: Fig. 6 shows 5:2 and 3:2 synchronization epochs.

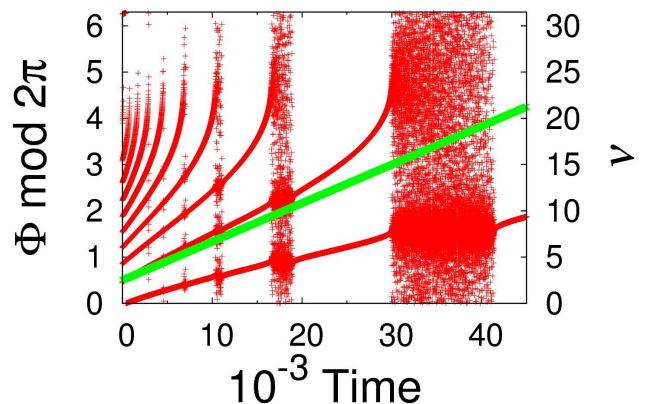


FIG. 5: (colour online). An $n:1$ synchrogram for the forced rotator while varying the driving frequency. Several $n:1$ synchronization epochs can be observed. The straight line plots the instantaneous frequency of the external driving (right-hand ordinate axis).

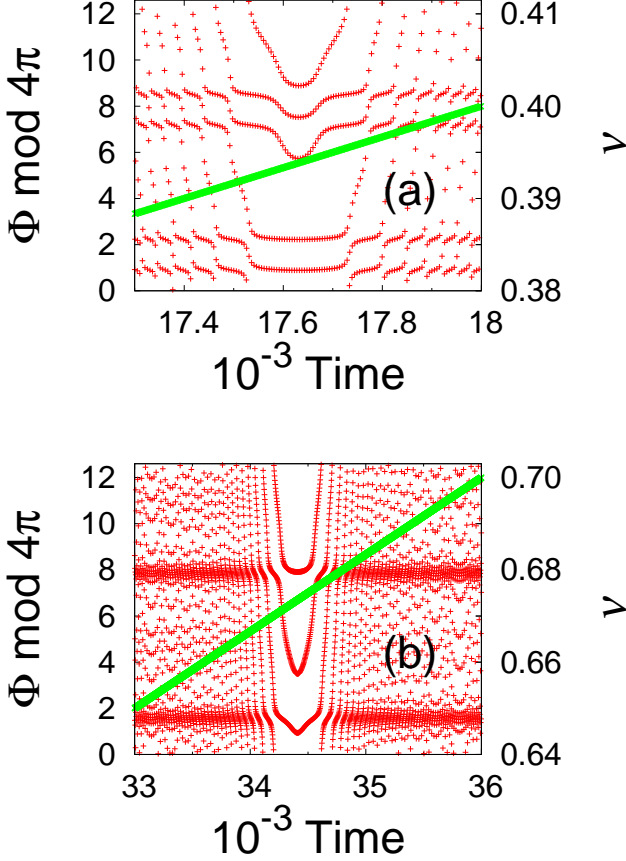


FIG. 6: (colour online). Sections of an $n:2$ synchrogram for the forced rotator while varying the driving frequency, illustrating a 5:2 synchronization epoch in (a) and a 3:2 epoch in (b). The straight line plots the instantaneous frequency of the external driving (right-hand ordinate axis).

For a Josephson junction, transitions of this kind could be induced by variation of the frequency of the harmonic component of the current driving the system. Where we regard (6) as a simple model for the heart driven by the respiration, the transition mechanism would correspond to variation of the respiration rate. Although this rate can be consciously controlled [25], people do not do so most of the time, and so the small natural variations in respiration rate can produce transitions in the synchronization ratio between it and the heart.

B. Low-frequency noise

The second transition mechanism considered here arises from the effect of the low-frequency noise that is often present in physical, biological and economic systems. For instance, flicker noise [26] occurs in almost all electronic devices. Another example is the cardiovascular system, where there are known to be metabolic,

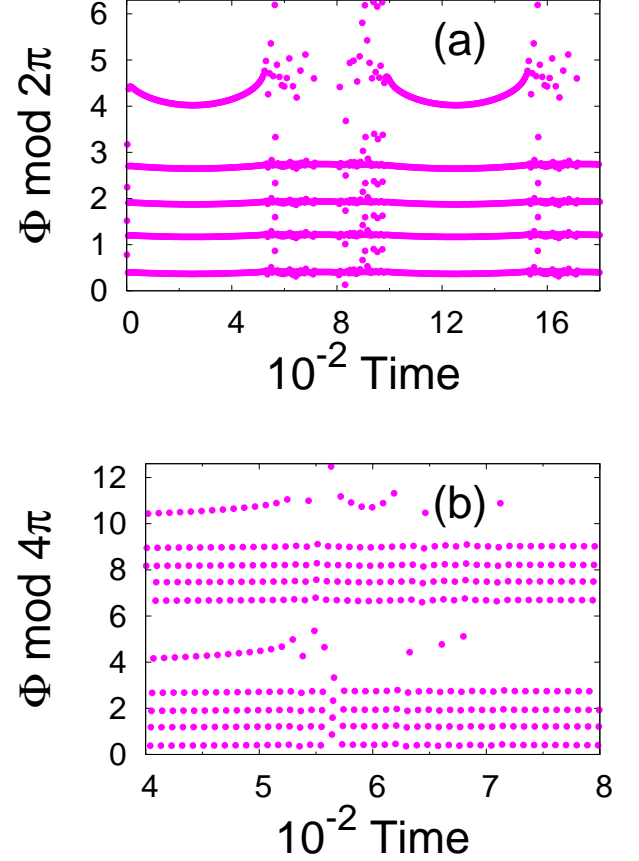


FIG. 7: (a) Transitions between 5:1 and 4:1 synchronization states, caused by the added low frequency component. (b) A 9:2 epoch for time ~ 600 in the transition between 5:1 and 4:1.

neurogenic and myogenic [27] low-frequency oscillatory processes.

We therefore added to our system an extra low-frequency harmonic component, simulating Eq. (6) with $(a_0, a_1) = (9.85714, 7.14286)$, $B=4$, $\omega/2\pi=0.213$, with a term $L_1 \sin(\omega_1 t)$ added to the RHS, $L_1=0.1$ and $\omega_1/2\pi=0.001$. This value of ω_1 may appear low compared to some natural systems, but the results we will obtain remain valid for larger ω_1 provided it is small compared with the frequencies of the other processes. Without adding the low frequency component, we would be inside the 5:1 tongue and the synchrogram would consist of 5 perfect horizontal lines. As shown in Fig. 7(a), the corresponding simulation exhibits transitions between 5:1 and 4:1. Note that we have added a harmonic low-frequency component; with low-frequency noise, the sequence of transitions will not be predictable in the manner seen here. In Fig. 7(b) we see a 9:2 epoch inside the transition region between the two longest epochs.

This second mechanism is mathematically equivalent to a slow variation of the intrinsic frequency of the rota-

tor. This can be seen by considering the low-frequency component to be absorbed inside a_0 , yielding an a_0 , and therefore a ν_0 , that slowly vary with time. In nature, however, the picture is completely different, as the low-frequency noise comes from *outside* the rotator.

C. Time variability and synchronization

Although we can still recognise synchronization epochs from the synchrograms by sight, time variability – the origin of the two transition mechanisms discussed above – means that synchrograms no longer consist of perfect horizontal lines. The test via a synchronization index, often used when tackling real experimental data, must fail, even inside a small time window, unless we take a less strict threshold for the index. Our result is in agreement with that obtained in [22] by analysis of experimental data. In short, time variability interferes with synchronization; at least for our system and with the index (8) as a quantification of synchronization. A more detailed and quantitative study of the influence of time variability is in progress and will be reported elsewhere.

V. CONCLUSIONS

We have shown that the driven rotator Eq. (6) yields a vast variety of Arnold tongues. Our results are applica-

ble to the several systems described by this equation, including the overdamped pendulum and the overdamped Josephson junction. Because the synchronization regions can be relatively wide, and because (1) is written in terms of continuous variables, the equation may be useful in modelling the wide range of high-order synchronization phenomena observed in nature, such as in the cardiorespiratory interaction. Although we investigate a specific system, and although the deep mechanisms for synchronization are not revealed by our studies in this paper, two of the results that we have obtained are very interesting and likely to be useful in the quest for those deep mechanisms: we showed that a strong dependence of the instantaneous frequency on the angle helps high-order synchronization; and we also identified and studied the phenomenon of competition among tongues. Finally, we have discussed and explored two mechanisms of transition between different synchronization states.

Acknowledgments

We thank A. Bahraminasab, A. Pikovsky and M. Rosenblum for useful discussions.

This work was supported by EU Project BRACCIA [28].

-
- [1] A. Pikovsky, M. Rosenblum and J. Kurths, *Synchronization. A Universal Concept in Nonlinear Sciences*. Cambridge University Press, 2001.
 - [2] J. Simonet, M. Warden and E. Brun, Phys. Rev. E **50**, 3383 (1994)
 - [3] A. K. Jain, K. K. Likharev, J. E. Lukens and J. E. Sauvageau, Phys. Reports **109**, 309–426 (1984)
 - [4] T. Kenner, H. Passenhofer and G. Schwabberger, Pflügers Archiv. **363**, 263–265 (1976); G. Hildebrandt, in *Temporal Disorder in Human Oscillatory System*, edited by L. Rensing, U. an der Heiden and M. C. Mackey (Springer, Berlin, 1987), pp. 160–174; F. Raschke, *ibid*, pp. 152–158; F. Raschke, in *Rhythms in Physiological Systems*, edited by H. Haken and H. P. Koepchen (Springer, Berlin, 1991), pp. 155–164.
 - [5] C. Schäfer, M.G. Rosenblum, J. Kurths and H.H. Abel, Nature (London) **392**, 239 (1998); M.G. Rosenblum *et al*, IEEE Eng. Med. Biol. Mag. **17**, 46 (1998); C. Schäfer, M.G. Rosenblum, H.H. Abel and J. Kurths, Phys. Rev. E **60**, 857 (1999)
 - [6] E. Toledo, S. Akselrod, I. Pinhas, D. Aravot, Med. Eng. and Phys. **24**, 45 (2002)
 - [7] A. Stefanovska, H. Haken, P.V.E. McClintock, M. Hožič, F. Bajrović and S. Ribarič, Phys. Rev. Lett. **85**, 4831 (2000); B. Musizza, A. Stefanovska, P.V.E. McClintock, M. Paluš, J. Petrovič, S. Ribarič and F. Bajrović, J. Physiol **580**.1, 315–326 (2007)
 - [8] V.I. Arnold, Usp. Mat. Nauk. **38** (4), 189–203 (1983) (In Russian); English translation: Russ. Math. Surveys **38**, 215–233 (1983)
 - [9] A. Katok and B. Hasselblatt, *Introduction to the Modern Theory of Dynamical Systems* (Cambridge University Press, Cambridge, 1995).
 - [10] P. L. Boyland, Commun. Math. Phys. **106**, 353–381 (1986)
 - [11] P. H. E. Tiesinga, Phys. Rev. E **65**, 041913 (2002); S. Coombes and P.C. Bressloff, Phys. Rev. E **60**, 2086 (1999)
 - [12] L. Glass and J. Sun, Phys. Rev. E **50**, 5077 (1994)
 - [13] F. Schilder and B.B. Peckham, J. Comp. Phys. **220**, 932–951 (2007)
 - [14] K. Kotani, K. Takamasu, Y. Ashkenazy, H.E. Stanley and Y. Yamamoto, Phys. Rev. E **65**, 051923 (2002)
 - [15] R.W. DeBoer, J.M. Karemaker and J. Strackee, Am. J. Physiol. **253**, 680 (1987)
 - [16] H. Seidel and H. Herzel, Physica D **115**, 145 (1998)
 - [17] Note that “rotator” and “angle” are different from “phase oscillator” and “phase”. The equation of motion of a phase oscillator in the limit cycle is, by definition of phase, $\dot{\phi} = \omega$ [1, 18].
 - [18] Y. Kuramoto, *Chemical Oscillations, Waves, and Turbulence*. Springer-Verlag, 1984.
 - [19] R. Adler, Proc. IRE **34**, 351–357 (1946). Reprinted in Proc. IEEE **61**, 1380–1385 (1973).
 - [20] In cardiovascular system recordings, the respiratory signal looks typically like that from a harmonic oscillator

plus higher harmonics. On the other hand, it is known that the coupling from respiration to heart is stronger than vice versa [21].

- [21] M. G. Rosenblum, L. Cimponeriu, A. Bezerianos, A. Patzak and R. Mrowka, Phys. Rev. E **65**, 041909 (2002); M. Paluš and A. Stefanovska, Phys. Rev. E **67**, 055201(R) (2003); V.N. Smelyanskiy, D.G. Luchinsky, A. Stefanovska and P.V.E. McClintock, Phys. Rev. Lett. **94**, 098101 (2005); J. Jamšek, A. Stefanovska, and P.V.E. McClintock, Phys. Med. Biol. **49**, 4407–4425 (2004); A. Bahraminasab, F. Ghasemi, A. Stefanovska, P.V.E. McClintock, and H. Kantz, Phys. Rev. Lett. **100**, 084101 (2008)
- [22] M. Bračič Lotrič and A. Stefanovska, Physica A **283**, 451–461 (2000)
- [23] To plot Fig. 3 we removed a small artifact: inside the wide tongues 5:1 and 4:1, some regions of multiples with the same ratio appeared. For example, inside the 5:1 tongue, some areas with 15:3, 20:4, etc. were obtained. These regions were merged by hand into the wide tongue for two reasons: first, because visual inspection of the plot of $\theta(t)$ together with the plot of the external forcing revealed that it was actually 5:1 (or 4:1) synchronization; second and more important, because according to [9, 10] the characteristic parameter of synchronization in a circle map is the rotation number n/m .
- [24] R. Bartsch, J. W. Kantelhardt, T. Penzel and S. Havlin, Phys. Rev. Lett. **98**, 054102 (2007)
- [25] S. Rzecziński, N. B. Janson, A. G. Balanov, and P. V. E. McClintock, Phys. Rev. E **66**, 051909 (2002)
- [26] A. van der Ziel, Proc. IEEE **76**, 233–258 (1988)
- [27] A. Stefanovska and M. Bračič, Contemporary Physics **40**, 31–55 (1999)
- [28] <http://www.lancs.ac.uk/depts/physics/braccia/>